

# Threshold zero-kinetic-energy photoelectron spectroscopy of the $a^3\Sigma^+$ state of $\text{NO}^+$

Kwanghsi Wang and V. McKoy

Arthur Amos Noyes Laboratory of Chemical Physics,<sup>a)</sup> California Institute of Technology, Pasadena, California 91125

(Received 6 September 1995; accepted 1 December 1995)

Results of calculations of the photoelectron spectra for single-photon pulsed-field ionization of the  $1\pi$  orbital of the  $X^2\Pi$  ( $v''=0$ ) ground state  $\text{NO}$  leading to the  $a^3\Sigma^+$  ( $v^+=0-2$ ) excited ionic state are reported. Agreement between these calculated and recently measured spectra is very encouraging. Comparison of these spectra for ionization of the  $1\pi$  level of  $\text{NO}$  ( $X^2\Pi$ ) with those for the  $2\pi$  orbital reveal significantly different spectral profiles and underlying dynamics for these two cases. © 1996 American Institute of Physics. [S0021-9606(96)01710-3]

## I. INTRODUCTION

Zero-kinetic-energy (ZEKE) photoelectron spectroscopy, based on pulsed-field ionization of high Rydberg states lying below an ion threshold, has made it possible to obtain rotationally resolved photoelectron spectra for a wide range of molecules.<sup>1,2</sup> Coupled with related theoretical studies, these state-resolved spectra have often provided significant insight into the underlying photoionization dynamics. For example, these spectra have served to highlight the nonatomiclike behavior of molecular photoelectrons and the role of Cooper minima.<sup>1,3</sup>

To date, most such rotationally resolved photoelectron spectra have been studied by resonance enhanced multiphoton ionization (REMPI) of Rydberg states or by single-photon ionization of jet-cooled ground state molecules by coherent vacuum ultraviolet (VUV) radiation. Furthermore, these studies have generally dealt with the lowest ionic state. Recently, however, Kong *et al.*<sup>4,5</sup> have reported ZEKE photoelectron spectra for the  $a^3\Sigma^+$  ( $1\pi^{-1}$ ) excited state of  $\text{NO}^+$  and the  $A^2\Pi$  excited state of  $\text{CO}^+$  ( $1\pi^{-1}$ ) resulting from ionization of the ground states of these molecules by coherent extreme vacuum ultraviolet (EUV) radiation. Such studies can provide new insight into the behavior of excited electronic states of molecular ions. We have previously reported calculated photoelectron spectra<sup>6</sup> for the  $A^2\Pi_{3/2}$  and  $A^2\Pi_{1/2}$  states of  $\text{CO}^+$  and a comparison of these spectra with the measured ZEKE spectra of Kong *et al.*<sup>5</sup>

In this paper we present calculated rotationally resolved ZEKE photoelectron spectra of the electronically excited  $a^3\Sigma^+$  state of  $\text{NO}^+$  for ionization of the  $1\pi$  orbital of  $\text{NO}$  by coherent EUV radiation. These calculated spectra, obtained assuming a Gaussian detection function with a full-width at half-maximum (FWHM) of  $3.5\text{ cm}^{-1}$ , the effective electron resolution of the measurements of Kong *et al.*,<sup>4</sup> agree quite well with the measured spectra. The spectra display some interesting differences from those for ionization of the  $2\pi$  level of  $\text{NO}$ . Comparison of the photoelectron spectra for this excited state of  $\text{NO}^+$ , calculated assuming an FWHM of  $1\text{ cm}^{-1}$ , with the results of similar calculations for the

ground ( $X^1\Sigma^+$ ) state of  $\text{NO}^+$ , further highlight these differences.

## II. THEORY AND NUMERICAL DETAILS

### A. Differential cross section

Under collision-free conditions, ionization originating from each of the  $(2J_0+1)$  magnetic sublevels of the initial state forms an independent channel. The total cross section  $\sigma$  for ionization of a  $J$  level of the initial state leading to a  $J^+$  level of the ion can then be written as

$$\sigma \propto \sum_{M_J, M_{J^+}} \rho_{M_J M_{J^+}} |C_{lm}(M_J, M_{J^+})|^2, \quad (1)$$

where  $\rho_{M_J M_{J^+}}$  is the population of a specific  $M_J$  level of the initial state. The coefficients  $C_{lm}(M_J, M_{J^+})$  of Eq. (1) are related to the probability for photoionization of the  $M_J$  level of the initial state leading to the  $M_{J^+}$  level of the ionic state. The  $C_{lm}(M_J, M_{J^+})$  coefficients, which explicitly consider the spin coupling associated with multiplet-specific final-state wave functions and a coupling scheme intermediate between Hund's cases (a) and (b) for the initial and ionic states, have the simple form:<sup>7</sup>

$$C_{lm}(M_J, M_{J^+}) = C' [1 + (-1)^Q] \left[ \sum \tilde{I}_{l\lambda\mu; \Sigma_e} G \begin{pmatrix} J^+ & J & J_t \\ -\Omega_+ & \Omega & \lambda_t \end{pmatrix} \times \begin{pmatrix} S_+ & S_e & S \\ \Sigma_+ & \Sigma_e & -\Sigma \end{pmatrix} + \tilde{I}_{l\lambda\mu; \Sigma_e} (-1)^P \times G \begin{pmatrix} J^+ & J & J_t \\ -\Omega_+ & -\Omega & \lambda_t \end{pmatrix} \begin{pmatrix} S_+ & S_e & S \\ \Sigma_+ & \Sigma_e & \Sigma \end{pmatrix} \right], \quad (2)$$

where

$$G = \begin{pmatrix} J_r & 1 & J_t \\ -\lambda_r & \mu & -\lambda_t \end{pmatrix} \begin{pmatrix} S_e & l & J_r \\ -\Sigma_e & -\lambda & \lambda_r \end{pmatrix}, \quad (3)$$

$$Q = \Delta J + \Delta S + 2S_e + \Delta p + l + 1, \quad (4)$$

<sup>a)</sup>Contribution No. 9133.

$$p = \begin{cases} 0 & \text{for } e \text{ states} \\ 1 & \text{for } f \text{ states} \end{cases} \quad (5)$$

and

$$\tilde{I}_{l\lambda\mu;\Sigma_e} = \sum_{\Lambda_f \Sigma_f} \langle \Lambda_+ \lambda | \Lambda_f \rangle \langle \Sigma_+ \Sigma_e | \Sigma_f \rangle I_{l\lambda\mu}(\Lambda_f \Sigma_f), \quad (6)$$

with  $\Delta J = J^+ - J$ ,  $\Delta S = S_+ - S$ ,  $\Delta p = p^+ - p$ . In Eq. (2),  $C'$  is a laboratory-frame quantity given in Ref. 7. In these equations,  $\Omega$  denotes the total electronic angular momentum about the internuclear axis,  $\Lambda$  the projection of electronic orbital angular momentum along the internuclear axis,  $S$  the total spin,  $\Sigma$  its projection along the internuclear axis,  $S_e$  the spin of the photoelectron,  $\Sigma_e$  its projection along the laboratory  $z$  axis and  $p$  the parity of each rotational level. For the branching ratios of interest here, the constant implied in Eq. (1) is unimportant and will be suppressed.

Equations (2) and (4) yield the parity selection rule<sup>7-9</sup>

$$\Delta J + \Delta S + 2S_e + \Delta p + l = \text{odd} \quad (7)$$

for photoionization of the ground state of NO. In the one-electron approximation, the photoelectron matrix elements of Eq. (6) for each dipole-allowed final-state wave function  $|\Lambda_f \Sigma_f\rangle$  can be written as (in the molecular frame)

$$I_{l\lambda\mu}(\Lambda_f \Sigma_f) = (-1)^l e^{i\eta_l} \langle \psi_{kl\lambda}(\mathbf{r}) | r Y_{1\mu} | \psi_i(\mathbf{r}) \rangle, \quad (8)$$

with  $\psi_{kl\lambda}$  the partial wave component of the photoelectron with momentum  $\mathbf{k}$  and  $\eta_l$  the Coulomb phase shift.<sup>10</sup>

## B. Multiplet-specific wave functions and potentials

There are three dipole-allowed channels for photoionization of the  $1\pi$  orbital of the  $X^2\Pi$  ground state of NO leading to the  $a^3\Sigma^+$  excited state of  $\text{NO}^+$ . The corresponding multiplet-specific final-state wave functions are given by

$$\begin{aligned} \Psi(^2\Sigma^+) = \frac{1}{\sqrt{12}} [ & 2|(\text{core})1\pi_+^2 1\pi_-^2 2\pi_-^1 \bar{k}\sigma| - |(\text{core})1\pi_+^2 1\pi_-^2 2\pi_-^1 k\sigma| - |(\text{core})1\pi_+^2 1\pi_-^2 2\pi_-^1 k\sigma| \\ & + 2|(\text{core})1\pi_-^2 1\pi_+^2 2\pi_+^1 \bar{k}\sigma| - |(\text{core})1\pi_-^2 1\pi_+^2 2\pi_+^1 k\sigma| - |(\text{core})1\pi_-^2 1\pi_+^2 2\pi_+^1 k\sigma| ], \end{aligned} \quad (9)$$

$$\begin{aligned} \Psi(^2\Pi) = \frac{1}{\sqrt{12}} [ & 2|(\text{core})1\pi_+^2 1\pi_-^2 2\pi_-^1 \bar{k}\pi_+| - |(\text{core})1\pi_+^2 1\pi_-^2 2\pi_-^1 k\pi_+| - |(\text{core})1\pi_+^2 1\pi_-^2 2\pi_-^1 k\pi_+| \\ & + 2|(\text{core})1\pi_-^2 1\pi_+^2 2\pi_+^1 \bar{k}\pi_+| - |(\text{core})1\pi_-^2 1\pi_+^2 2\pi_+^1 k\pi_+| - |(\text{core})1\pi_-^2 1\pi_+^2 2\pi_+^1 k\pi_+| ], \end{aligned} \quad (10)$$

and

$$\begin{aligned} \Psi(^2\Delta) = \frac{1}{\sqrt{12}} [ & 2|(\text{core})1\pi_+^2 1\pi_-^2 2\pi_-^1 \bar{k}\delta_+| - |(\text{core})1\pi_+^2 1\pi_-^2 2\pi_-^1 k\delta_+| - |(\text{core})1\pi_+^2 1\pi_-^2 2\pi_-^1 k\delta_+| \\ & + 2|(\text{core})1\pi_-^2 1\pi_+^2 2\pi_+^1 \bar{k}\delta_+| - |(\text{core})1\pi_-^2 1\pi_+^2 2\pi_+^1 k\delta_+| - |(\text{core})1\pi_-^2 1\pi_+^2 2\pi_+^1 k\delta_+| ], \end{aligned} \quad (11)$$

with  $(\text{core}) = 1\sigma^2 2\sigma^2 3\sigma^2 4\sigma^2 5\sigma^2$  and the bars over the orbitals indicate opposite spin.

Within the frozen-core Hartree-Fock model, the one-electron Schrödinger equation for the photoelectron orbital  $\phi_k$  associated with such final-state wave functions can be shown to have the form<sup>10</sup>

$$P \left( f + \sum_{i=\text{core}} (2J_i - K_i) + a_n J_n + b_n K_n - \epsilon \right) P | \phi_k \rangle = 0, \quad (12)$$

where  $J_i$  and  $K_i$  are the Coulomb and exchange operators, respectively, and  $P$  is a projection operator which enforces orthogonality of the continuum orbital to the occupied orbitals. The photoelectron kinetic energy is given by  $\epsilon = (1/2)k^2$ . The one-electron operator  $f$  in Eq. (12) is

$$f = -\frac{1}{2} \nabla_i^2 - \sum_{\alpha} \frac{Z_{\alpha}}{r_{i\alpha}}, \quad (13)$$

where  $Z_{\alpha}$  is a nuclear charge. For the final-state wave functions of Eqs. (9)–(11), the coefficient  $a_n$  and  $b_n$  associated with the  $1\pi$  orbital assume values of  $3/2$  and  $-1/4$ , respectively. The corresponding values for the  $2\pi$  orbital are  $1/2$  and  $1/4$ .

## C. Numerical details

The ground state wave function of NO used here is obtained at the self-consistent-field (SCF) level. We used the same basis sets as in Ref. 11 for the ground state wave functions of NO for 12 internuclear distances between 1.95 and 2.8  $a_0$ . The vibrational wave functions for the  $X^2\Pi$  ground state of NO and the  $a^3\Sigma^+$  excited state of  $\text{NO}^+$  were obtained by numerical integration over this range using our calculated potential curves. The calculated dipole moment for the  $a^3\Sigma^+$  excited state of  $\text{NO}^+$  with origin at the center-of-mass is  $-0.207$  a.u. The single-center expansion of the  $1\pi$  orbital about the center-of-mass has 78.55%  $p$ , 2.80%  $d$ ,

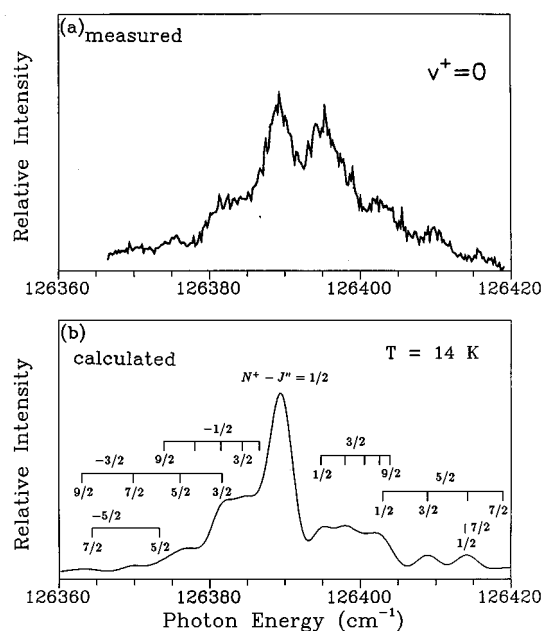


FIG. 1. (a) Measured and (b) calculated rotationally resolved threshold PFI photoelectron spectra for the single-photon ionization transition  $\text{NO}^+[a^3\Sigma^+(v^+=0, N^+)] + e^- \leftarrow \text{NO}[X^2\Pi_{1/2}(v''=0, J'')]$ . The rotational branch labels refer to  $N^+ - J''$ .

15.80%*f*, 0.43%*g* ( $l_0=4$ ), and 1.88%*h* ( $l_0=5$ ) character. Further details of the calculations can be found in Refs. 11 and 12.

### III. RESULTS AND DISCUSSION

Our calculated near-threshold (ZEKE) photoelectron spectra for the  $v^+=0, 1$ , and 2 levels of the  $a^3\Sigma^+$  state of  $\text{NO}^+$  are shown in Figs. 1(b), 2(b), and 3(b), respectively. The spectra were obtained for a rotational temperature of 14 K. This temperature gave the most satisfactory agreement with the measured ZEKE spectra of Kong *et al.*,<sup>4</sup> shown in Figs. 1(a)–3(a), and is quite close to the measured (by REMPI) rotational temperature of about 10 K. These spectra were calculated for a photoelectron energy of 50 meV and convoluted with a Gaussian detection function with a full-width at half-maximum (FWHM) of 3.5  $\text{cm}^{-1}$ . The branches are labeled as  $N^+ - J''$ , where  $N^+$  is the quantum number for the nuclear rotation of the ion and  $J''$  is the total angular momentum of the ground state neutral molecule. The calculated spectra for  $v^+=1$  [Fig. 2(b)] and 2 [Fig. 3(b)] agree quite well with the measured spectra.

The calculated threshold photoionization spectra for  $v^+=0-2$  levels are essentially identical to one another. This is expected since the photoelectron matrix elements do not have a significant dependence on internuclear distance. On the other hand, non-Franck–Condon behavior has been seen in the measured spectra and results in an unusually strong intensity for the  $v^+=1$  level.<sup>4</sup> However, our calculated intensities do not display such behavior. This unusual intensity has been attributed to a complex resonance arising from an interloper Rydberg state with low principal quantum number

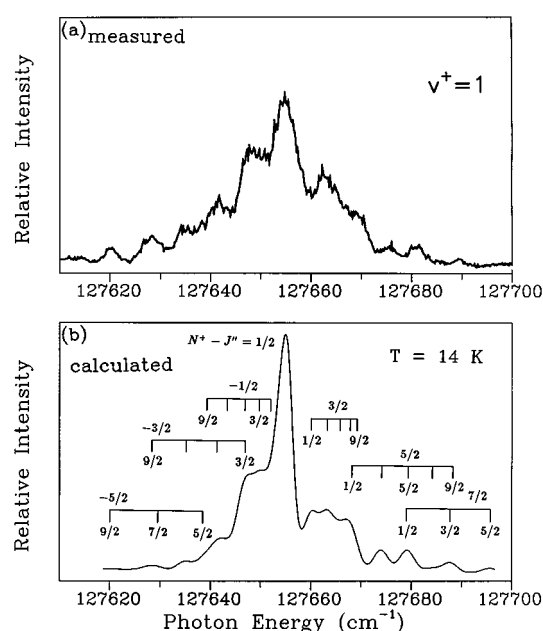


FIG. 2. (a) Measured and (b) calculated rotationally resolved threshold PFI photoelectron spectra for the single-photon ionization transition  $\text{NO}^+[a^3\Sigma^+(v^+=1, N^+)] + e^- \leftarrow \text{NO}[X^2\Pi_{1/2}(v''=0, J'')]$ . The rotational branch labels refer to  $N^+ - J''$ .

and strong oscillator strength. Indeed, a 5*p* Rydberg level converging to the  $b^3\Pi$  ( $v=0$ ) state, is almost resonant (30  $\text{cm}^{-1}$  apart) with this  $v^+=1$  level.<sup>4,13</sup> The calculated and measured spectra in Figs. 2(a) and 2(b) suggest that this complex resonance does not influence the rotational spectral

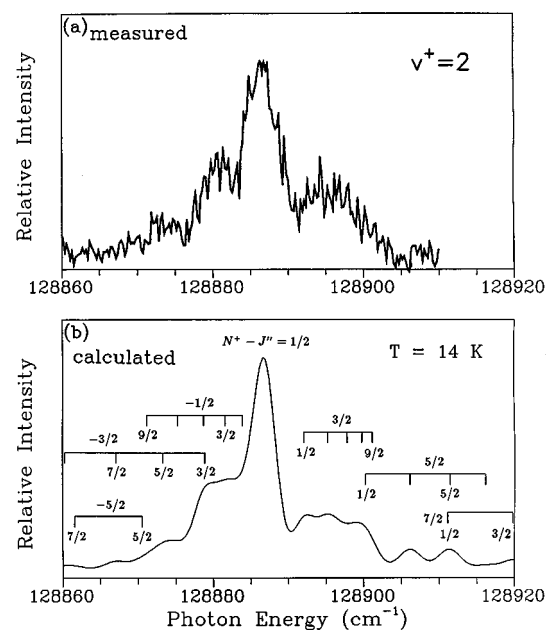


FIG. 3. (a) Measured and (b) calculated rotationally resolved threshold PFI photoelectron spectra for the single-photon ionization transition  $\text{NO}^+[a^3\Sigma^+(v^+=2, N^+)] + e^- \leftarrow \text{NO}[X^2\Pi_{1/2}(v''=0, J'')]$ . The rotational branch labels refer to  $N^+ - J''$ .

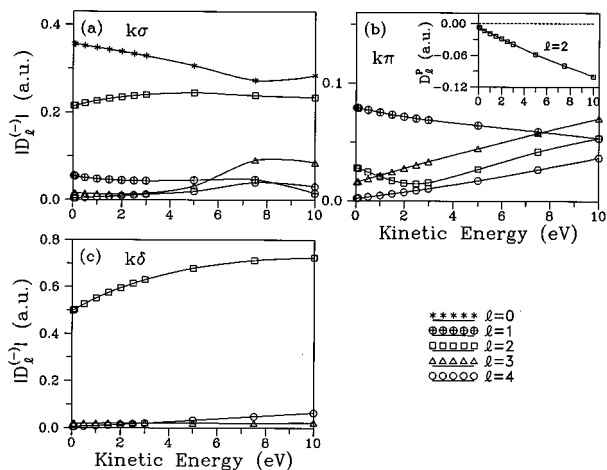


FIG. 4. Magnitude of the partial wave components of the photoelectron matrix element  $|D_l^{(-)}|$  for photoionization of the  $X^2\Pi$  ground state of NO leading to the  $a^3\Sigma^+$  excited state of  $\text{NO}^+$ . (a)  $1\pi \rightarrow k\sigma$ ; (b)  $1\pi \rightarrow k\pi$ ; and (c)  $1\pi \rightarrow k\delta$  ionization channels.

profiles. Furthermore, comparison of the measured and calculated  $v^+=0$  spectra reveals a perturbation of the intensity distribution of the observed rotational branches around  $N^+ - J''=3/2$  ( $J''=1/2$ ) region. Similar behavior has also been seen in the threshold photoelectron spectrum for photoionization of the  $2\pi$  orbital of the  $X^2\Pi$  ground state NO, where abnormal intensity in the rotational distributions for the  $v^+=0$  level of the ion is attributed to perturbations involving low  $n$  Rydberg states,<sup>14-16</sup> e.g., the  $8s, v=1$  level of NO (Ref. 11). The current intensity perturbations may result from similar isolated autoionizing resonances.

Parity selection rules,<sup>7-9</sup> governing changes of rotational angular momentum upon ionization, have been derived previously. Since the  $\Lambda$  doublets ( $e/f$ ) of the  $X^2\Pi_{1/2}$  ground state rotational levels are not resolved, it is not possible to assign a specific parity to individual rotational transitions as was the case for REMPI measurements via several  $2\Sigma^+$  Rydberg states of NO.<sup>12,17-21</sup> Therefore, both parity components of the  $\Lambda$  doublet, associated with either even or odd photoelectron partial waves, can contribute to each rotational transition. To provide some additional dynamical insight into these spectra, we show the calculated magnitudes  $|D_l^{(-)}|$  of the (incoming-wave normalized) partial wave components of the photoionization matrix element as a function of photoelectron kinetic energy in Fig. 4. Note that  $|D_l^{(-)}|$  is the magnitude of only one of the  $\mu$  components of  $I_{l\lambda\mu}$  [see Eq. (8)]. Near threshold, these calculated  $|D_l^{(-)}|$ 's show that the  $s$  ( $l=0$ ) and  $d$  ( $l=2$ ) partial waves of the  $k\sigma$  and  $k\delta$  continua, respectively, and the  $p$  ( $l=1$ ) wave of the  $k\pi$  channel account for a substantial portion of the photoionization cross section. Since the  $1\pi$  orbital of the  $X^2\Pi$  ground state of NO has almost pure odd wave [79% $p$ , 16% $f$ , and 2% $h$  ( $l_0=5$ )] character, dominant even partial wave contributions to the photoelectron matrix elements are expected on the basis of an atomiclike propensity rule. The unusually strong  $p$  wave seen in the  $k\pi$  continuum [Fig. 4(b)] indicates that the mo-

lecular photoionization dynamics is quite non-atomiclike.

Evidence of a Cooper minimum<sup>22</sup> in the  $d$  ( $l=2$ ) component of the photoelectron matrix element  $|D_l^{(-)}|$  is seen around 2.2 eV in the  $k\pi$  channel. The actual sign change in the dipole matrix element occurs in the principle-value (standing-wave normalized) dipole amplitude  $D_l^P$ , as shown in the inset of the Fig. 4(b).<sup>23</sup> Since the photoionization oscillator strengths is continuous across the ionization threshold, this behavior indicates that a Cooper zero may occur in the discrete spectral region. The energy position of the minimum in  $|D_l^{(-)}|$  differs somewhat from that of Cooper zero in  $D_l^P$ . This shift reflects the influence of angular momentum coupling in the electronic continua on the transformation relating  $D_l^P$  and  $D_l^{(-)}$ . The depletion of the  $d$  wave contribution to the photoelectron matrix element in the vicinity of this Cooper minimum subsequently enhances the relative importance of the odd waves. Due to the broad effects of Cooper minima, this Cooper minimum in the  $k\pi$  channel could exert some influence on the threshold photoionization.

Wiedmann *et al.*<sup>11</sup> have measured threshold photoelectron spectra for photoionization of the  $2\pi$  orbital of the  $X^2\Pi_{1/2}$  ground state of NO leading to the  $X^1\Sigma^+(v^+=0,1)$  ground ionic state. Only small changes in total angular momentum were observed ( $|\Delta J| \leq 5/2$ ) with branch intensities falling off rapidly as  $|\Delta J|$  increases. Theoretical studies revealed significant  $d$  ( $l=2$ ) and  $f$  ( $l=3$ ) partial wave contributions to the photoelectron matrix elements which, on the basis of angular momentum conservation, could result in large changes in angular momentum. The absence of large  $|\Delta J|$  peaks has been attributed to interference between partial waves in the photoelectron continua. On the other hand, changes in angular momentum up to  $|N^+ - J''|=7/2$  are seen in the threshold photoelectron spectra for photoionization of the  $1\pi$  orbital of the  $X^2\Pi_{1/2}$  ground state leading to the  $a^3\Sigma^+(v^+=0-3)$  excited ionic state. As discussed above, the  $d$  ( $l=2$ ) wave is the highest one making a significant contribution to the photoelectron matrix element. Angular momentum conservation limits  $|\Delta J|$  to  $l+3/2$  or  $7/2$  ( $|N^+ - J''|=7/2$ ) in this case.

To explore such differences in photoionization of the  $1\pi$  and  $2\pi$  orbitals of the  $X^2\Pi$  state, we show the calculated threshold photoelectron spectra for photoionization of the  $1\pi$  [Fig. 5(a)] and the  $2\pi$  [Fig. 5(b)] orbitals of the  $X^2\Pi$  ground state of NO leading to the  $a^3\Sigma^+$  excited and the  $X^1\Sigma^+$  ground ionic states, respectively, at a temperature of 14 K. These spectra were calculated for a photoelectron energy of 50 meV and convoluted with a Gaussian detection function with an FWHM of  $1 \text{ cm}^{-1}$ . Clearly, dramatically different spectral profiles are obtained for photoionization of these  $\pi$  orbitals. Since both the even and odd partial waves contribute to each rotational transition, these photoelectron spectra should not depend much on the even or odd character of the initial  $\pi$  orbitals.

Some of the observed differences in the spectral profiles of Fig. 5 may be due to spectroscopic differences between these two states of the ion. To highlight the real underlying differences in their ionization dynamics, we compare branching ratios for  $N^+$  levels of both states for ionization out of

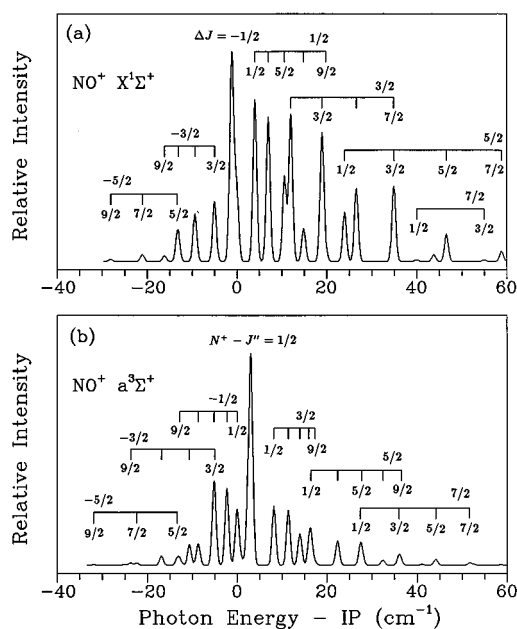


FIG. 5. Calculated rotationally resolved threshold PFI photoelectron spectra for single-photon ionization of the  $2\pi$  and  $1\pi$  orbitals of the  $X^2\Pi$  ground state of NO leading to the (a)  $X^1\Sigma^+$  and (b)  $a^3\Sigma^+$  ionic states, respectively. A rotational temperature of 14 K is assumed.

the  $J''=5/2$ ,  $N''=2$  level of the  $X^2\Pi_{1/2}$  component of the neutral molecule. These ratios are 0.157:0.560:0.854:1.000:0.861:0.322:0.011 for the  $X^1\Sigma^+$  ground state of the ion and 0.082:0.351:0.914:1.000:0.535:0.234:0.099 for the  $a^3\Sigma^+$  state for  $-2 \leq \Delta N \leq 4$  levels, respectively. Almost equal intensities for the  $\Delta N=0$  and  $\Delta N=2$  transitions are seen for the  $X$  state but not for the  $a$  state. On the other hand, these ratios are 0.244:0.589:0.857:1.000:0.668:0.186:0.006 for the  $X$  state and 0.092:0.527:1.000:0.815:0.410:0.184:0.058 for the  $a$  state for ionization of the  $J''=5/2$ ,  $N''=3$  level of the other spin-orbit component of the ground state of NO. The most intense peaks in the ion distributions are for different  $\Delta N$  transitions. These ion distributions simply reflect differences in the underlying photoelectron matrix elements.

## ACKNOWLEDGMENTS

This work was supported by grants from the Air Force Office of Scientific Research and the Office of Health and Environmental Research of the U.S. Department of Energy. We also acknowledge use of resources of the Jet Propulsion Laboratory/California Institute of Technology Y-MP2E/232 Supercomputer.

- <sup>1</sup> See, for example, the Wiley Series in Ion Chemistry and Physics, *High Resolution Laser Photoionization and Photoelectron Studies*, edited by I. Powis, T. Baer, and C.-Y. Ng (Wiley, New York, 1995).
- <sup>2</sup> K. Müller-Dethlefs and E. W. Schlag, *Annu. Rev. Phys. Chem.* **42**, 109 (1991).
- <sup>3</sup> K. Wang, J. A. Stephens, and V. McKoy, *J. Phys. Chem.* **97**, 9874 (1993).
- <sup>4</sup> W. Kong, D. Rodgers, and J. W. Hepburn, *J. Chem. Phys.* **99**, 8571 (1993).
- <sup>5</sup> W. Kong and J. W. Hepburn, *J. Phys. Chem.* **99**, 1637 (1995).
- <sup>6</sup> K. Wang and V. McKoy, *J. Phys. Chem.* **99**, 1643 (1995).
- <sup>7</sup> K. Wang and V. McKoy, *J. Chem. Phys.* **95**, 4977 (1991).
- <sup>8</sup> S. N. Dixit and V. McKoy, *J. Chem. Phys.* **82**, 3546 (1985).
- <sup>9</sup> J. Xie and R. N. Zare, *J. Chem. Phys.* **93**, 3033 (1990).
- <sup>10</sup> R. R. Lucchese, G. Raseev, and V. McKoy, *Phys. Rev. A* **25**, 2572 (1982).
- <sup>11</sup> R. T. Wiedmann, M. G. White, K. Wang, and V. McKoy, *J. Chem. Phys.* **98**, 7673 (1993).
- <sup>12</sup> K. Wang, J. A. Stephens, and V. McKoy, *J. Chem. Phys.* **95**, 6456 (1991).
- <sup>13</sup> P. H. Metzger, G. R. Cook, and M. Ogawa, *Can. J. Phys.* **45**, 203 (1967).
- <sup>14</sup> R. T. Wiedmann, E. R. Grant, R. G. Tonkyn, and M. G. White, *J. Chem. Phys.* **95**, 746 (1991).
- <sup>15</sup> R. T. Wiedmann, R. G. Tonkyn, M. G. White, K. Wang, and V. McKoy, *J. Chem. Phys.* **97**, 768 (1992).
- <sup>16</sup> R. G. Tonkyn, R. T. Wiedmann, and M. G. White, *J. Chem. Phys.* **96**, 3696 (1992).
- <sup>17</sup> W. G. Wilson, K. S. Viswanathan, E. Sekreta, and J. P. Reilly, *J. Phys. Chem.* **88**, 672 (1984); K. S. Viswanathan, E. Sekreta, E. R. Davidson, and J. P. Reilly, *ibid.* **90**, 5078 (1986); K. S. Viswanathan, E. Sekreta, and J. P. Reilly, *ibid.* **90**, 5658 (1986).
- <sup>18</sup> X. Song, E. Sekreta, J. P. Reilly, H. Rudolph, and V. McKoy, *J. Chem. Phys.* **91**, 6062 (1989).
- <sup>19</sup> S. W. Allendorf, D. J. Leahy, D. C. Jacobs, and R. N. Zare, *J. Chem. Phys.* **91**, 2216 (1989).
- <sup>20</sup> H. Rudolph and V. McKoy, *J. Chem. Phys.* **91**, 2235 (1989).
- <sup>21</sup> M. Sander, L. A. Chewter, K. Müller-Dethlefs, and E. W. Schlag, *Phys. Rev. A* **36**, 4543 (1987).
- <sup>22</sup> J. W. Cooper, *Phys. Rev.* **128**, 681 (1962); U. Fano and J. W. Cooper, *Rev. Mod. Phys.* **40**, 441 (1968); S. T. Manson, *Phys. Rev. A* **31**, 3698 (1985); A. Z. Msezane and S. T. Manson, *Phys. Rev. Lett.* **48**, 473 (1982).
- <sup>23</sup> J. A. Stephens and V. McKoy, *J. Chem. Phys.* **93**, 7863 (1990).